EJN European Journal of Neuroscience

FENS Federation of European Neuroscience Societies

European Journal of Neuroscience, Vol. 43, pp. 1366–1378, 2016 doi:10.1111/ejn.13191

MOLECULAR AND SYNAPTIC MECHANISMS

Microglia-derived purines modulate mossy fibre synaptic transmission and plasticity through $P2X_4$ and A_1 receptors

Jimmy George,[1,2,3] Rodrigo A. Cunha,[2,3] Christophe Mulle[1] and Thierry Amédée[1,4]
[1]Interdisciplinary Institute for Neuroscience, CNRS UMR 5297, University of Bordeaux, Bordeaux, France
[2]CNC Centre for Neuroscience and Cell Biology, University of Coimbra, Coimbra, Portugal
[3]Faculty of Medicine, University of Coimbra, Coimbra, Portugal
[4]IINS, UMR 5297 CNRS – Université de Bordeaux, Bordeaux Cedex, France

Keywords: A_1 receptor, hippocampal synaptic plasticity, microglia, $P2X_4$ receptor, purines

Edited by Gianmaria Maccaferri
Received 12 November 2015, accepted 21 January 2016

Abstract

Recent data have provided evidence that microglia, the brain-resident macrophage-like cells, modulate neuronal activity in both physiological and pathophysiological conditions, and microglia are therefore now recognized as synaptic partners. Among different neuromodulators, purines, which are produced and released by microglia, have emerged as promising candidates to mediate interactions between microglia and synapses. The cellular effects of purines are mediated through a large family of receptors for adenosine and for ATP (P2 receptors). These receptors are present at brain synapses, but it is unknown whether they can respond to microglia-derived purines to modulate synaptic transmission and plasticity. Here, we used a simple model of adding immune-challenged microglia to mouse hippocampal slices to investigate their impact on synaptic transmission and plasticity at hippocampal mossy fibre (MF) synapses onto CA3 pyramidal neurons. MF–CA3 synapses show prominent forms of presynaptic plasticity that are involved in the encoding and retrieval of memory. We demonstrate that microglia-derived ATP differentially modulates synaptic transmission and short-term plasticity at MF–CA3 synapses by acting, respectively, on presynaptic $P2X_4$ receptors and on adenosine A_1 receptors after conversion of extracellular ATP to adenosine. We also report that $P2X_4$ receptors are densely located in the mossy fibre tract in the dentate gyrus–CA3 circuitry. In conclusion, this study reveals an interplay between microglia-derived purines and MF–CA3 synapses, and highlights microglia as potent modulators of presynaptic plasticity.

Introduction

Microglia are brain-resident macrophage-like cells of the central nervous system, and have been recently acknowledged as synaptic partners (Ben Achour & Pascual, 2010; Tremblay *et al.*, 2010; Kettenmann *et al.*, 2013). Microglia modulate neuronal activity in both physiological and pathophysiological conditions (Bessis *et al.*, 2007; Roumier *et al.*, 2008; Wake *et al.*, 2009) through signalling mechanisms that are largely unknown. Purines are candidate signals, as microglia can release ATP (Pascual *et al.*, 2012; George *et al.*, 2015), which modulates synaptic transmission and plasticity (Neary & Zimmermann, 2009; Verkhratsky *et al.*, 2009; Burnstock *et al.*, 2011; Rodrigues *et al.*, 2015).

ATP has pleiotropic effects in the brain, which depend on different types of purinergic receptors expressed by neurons and glial cells, but also on its degradation by extracellular ectonucleotidases to adenosine (Burnstock *et al.*, 2011; Rodrigues *et al.*, 2015). Purinergic receptors are divided into two families activated either by adenosine (P1 receptors) or by ATP (P2 receptors). P1 receptors are G-protein-coupled, and comprise four different subtypes: A_1, A_{2A}, A_{2B}, and A_3 (Fredholm *et al.*, 2011). The P2 receptor family is subdivided in two subfamilies: the ionotropic P2X receptors (P2X receptors 1–7) family linked to increased cation permeability, and the metabotropic P2Y receptors (eight different subtypes) family coupled to G-proteins (Burnstock *et al.*, 2011).

P1 and P2 receptors are widely distributed at brain synapses. In the hippocampus, A_1 receptors (A_1Rs) are located at both presynaptic and postsynaptic loci (Rebola *et al.*, 2003), whereas A_{2A} receptors (A_{2A}Rs) are mostly presynaptic (Rebola *et al.*, 2005), but are also present in astrocytes (Matos *et al.*, 2012) and microglia (Rebola *et al.*, 2011). Adenosine decreases glutamatergic transmission via presynaptic A_1Rs (Dunwiddie & Masino, 2001), whereas it activates A_{2A}Rs to facilitate AMPA and *N*-methyl-D-aspartate receptor-mediated currents (Rebola *et al.*, 2008; Dias *et al.*, 2012) to modulate synaptic plasticity (Rebola *et al.*, 2008; Costenla *et al.*, 2011).

P2X receptors also modulate hippocampal synaptic transmission and plasticity (Pankratov *et al.*, 2002). Presynaptic $P2X_2$ receptors facilitate CA3 excitatory transmission onto interneurons in the CA1 region (Khakh *et al.*, 2003), whereas $P2X_4$ receptors ($P2X_4$Rs) tune the *N*-methyl-D-aspartate receptor-dependent component of long-term

Correspondence: Thierry Amédée, [4]IINS, as above.
E-mail: thierry.amedee@u-bordeaux.fr

plasticity at the Schaffer–collateral CA1 synapse (Sim *et al.*, 2006). This is in accordance with the expression of $P2X_2$, $P2X_3$, $P2X_4$ and $P2X_6$ receptor subunits by hippocampal neurons (Rodrigues *et al.*, 2005), whereas $P2X_7$ receptors are mostly expressed by activated glial cells (Butt, 2011).

In this study, we investigated the role of microglia–purine interactions at hippocampal synapses between mossy fibres (MFs) and CA3 pyramidal cells. MF-CA3 synapses show prominent forms of presynaptic plasticity (Marchal & Mulle, 2004; Nicoll & Schmitz, 2005), and are instrumental in the encoding and retrieval of memories (Nakazawa *et al.*, 2003; Bischofberger *et al.*, 2006; Kesner, 2007). We report that ATP and adenosine, derived from lipopolysaccharide (LPS)-challenged microglia (George *et al.*, 2015), do modulate synaptic transmission and short-term plasticity at MF-CA3 synapses by acting, respectively, on $P2X_4$Rs and A_1Rs. This study reveals an interplay between microglia and MF-CA3 synapses, and further supports microglia as true modulators of neuronal network through purinergic modulation of presynaptic function.

Materials and methods

Ethical approval

Experiments were carried out in accordance with the guidelines on the ethical use of animals from the European Communities Council Directive (86/609/EEC) and were evaluated by the Ethics commitee n°50 of Bordeaux, affiliated with the CNREEA (Centre National de Réflexion Ethique sur l'Expérimentation Animale).

Microglial cell culture and pharmacological treatment

A murine microglial cell line, N9 (a gift from C. Verderio, CNR Institute of Neuroscience, Cellular and Molecular Pharmacology, Milan, Italy), was grown in RPMI-1640 (Sigma, St Quentin Fallavier, France) medium supplemented with 30 mM glucose (Sigma), 5% heat-inactivated fetal bovine serum (Gibco, Invitrogen, Merelbeke, Belgium), 100 μg/mL streptomycin, and 1 U/mL penicillin (Gibco, Invitrogen). Cells were kept at 37 °C under a humidified atmosphere with 95% O_2 and 5% CO_2. In order to trigger microglia activation and ATP release, N9 cells were challenged with 100 ng/mL LPS (from *Escherichia coli*, serotype 055:B5; Sigma) for 1 h, which we have found to trigger ATP release and upregulation of A_{2A}Rs (Gomes *et al.*, 2013).

Slice preparation

C57BL6/J mice (Janvier Labs, Le Genest St Isle, France) were killed at postnatal day (P)19–P21 by cervical dislocation. The brain was then quickly removed from the skull, and chilled in ice-cold low-calcium artificial cerebrospinal fluid containing 87 mM NaCl, 2.5 mM KCl, 1.25 mM NaH_2PO_4, 0.5 mM $CaCl_2$, 7 mM $MgCl_2$, 10 mM glucose, 25 mM $NaHCO_3$, and 75 mM sucrose, adjusted to pH 7.4 by saturating with carbogen (95% O_2 and 5% CO_2), and with an osmolarity of 300–310 mOsm. Brains were then glued onto the stage of a vibratome (VT 1200S; Leica, Nusslich, Germany), and parasagittal hippocampal slices (320 μm) were cut. Slices were then transferred to an extracellular solution containing 129 mM NaCl, 2.5 mM KCl, 1.25 mM NaH_2PO_4, 2 mM $CaCl_2$, 1 mM $MgCl_2$, 11 mM glucose, and 25 mM $NaHCO_3$, equilibrated with carbogen for 30 min at 33 °C and thereafter at room temperature, until being used.

Electrophysiology

The slices were submerged in a recording chamber and continuously superfused with carbogen-saturated extracellular solution at 32–34 °C. Whole cell patch clamp recordings were made at a holding potential of −70 mV with electrodes of 3–4 MΩ. Patch clamp electrodes were pulled out from borosilicate glass (GF 150 F-10; Clark Electromedical, Reading, UK), and filled with an internal solution containing 140 mM $CsCH_3SO_3$, 2 mM $MgCl_2$, 4 mM NaCl, 5 mM phosphocreatine, 2 mM Na_2ATP, 0.2 mM EGTA, 10 mM HEPES, and 0.33 mM GTP (pH 7.3), adjusted with CsOH. Bicuculline (10 μM) was added to the bath to inhibit $GABA_A$ receptors.

Voltage-clamp recordings were performed on CA3 pyramidal neurons visualized with a differential interference contrast microscope (Eclipse FN-1; Nikon, Champigny sur Marne, France) equipped with an infrared camera (VX44; Till Photonics, Gräfelfing, Germany), by use of an Axoptach-200B amplifier (Axon Instruments, Sunnydale, CA, USA). Signals were filtered at 2 kHz and digitized at 5 kHz via a DigiData 1322A interface (Axon Instruments). Series resistance (10–20 MΩ) was monitored during the recording with a −10 mV hyperpolarizing voltage step (length, 50 ms) delivered at the beginning of each recording. Neurons were rejected if the series resistance changed by >20% during the experiment. Neurons with a holding current of >300 pA at a holding potential of −70 mV were rejected. Data were collected and analysed with PCLAMP software 9.2 (Axon Instruments). N9 microglia were challenged with LPS (100 ng/mL) for 1 h or not challenged, before being added to the slices. The cells were trypsinized and collected, and then added to a hippocampal slice at a density of ~100 000 cells per slice. N9 cells were allowed to adhere to the slices for 15–20 min, and the unattached cells were washed away, leaving approximately 400–500 cells stuck at the slice surface. Voltage-clamp recordings were obtained from CA3 pyramidal cells surrounded (10–100 μm) by three to five N9 cells in close vicinity. Excitatory postsynaptic currents (EPSCs) from MF–CA3 synapses were evoked by minimal-intensity stimulation of MFs (Marchal & Mulle, 2004; Sachidhanandam *et al.*, 2009). A glass electrode, with a tip diameter of ~1 μm, was placed on the hilus of the dentate gyrus to stimulate MFs. The baseline stimulation frequency for all experiments was 0.1 Hz. EPSCs were identified according to the following criteria: robust low-frequency facilitation, low release probability at low stimulation (0.1 Hz), rapid rise time of individual EPSCs, and being free of secondary peaks during decay. LCCG-1 (10 μM), a metabotropic glutamate receptor 2 agonist, was added routinely to confirm the selective stimulation of MFs, and cells were excluded if the inhibition was <80%. Pyridoxalphosphate-6-azophenyl-2′,4′-disulfonic acid (PPADS), ivermectin, 5-(3-bromophenyl)-1,3-dihydro-2*H*-benzofuro[3,2-e]-1,4-diazepin-2-one (5-BDBD), apyrase, ARL67156 and SCH58261 were obtained from Tocris (Bristol, UK), and 8-cyclopentyl-1,3-dipropylxanthine (DPCPX) and 2-chloro-N^6-cyclopentyladenosine (CCPA) were obtained from Abcam (Cambridge, UK). The antibody used for staining $P2X_4$Rs (Ref. HPA039494) was obtained from Atlas Antibodies (Stockholm, Sweden).

Immunohistochemistry

Mice (P19–P21) were anaesthetized by intraperitoneal administration of pentobarbital (50 mg/kg body weight), and were fixed by transcardial perfusion with 50 mL of 4% paraformaldehyde. Brains were removed and postfixed in 4% paraformaldehyde overnight, and then saturated in a solution with 30% sucrose for 24 h. They were then frozen in cold heptane, and stored at −80 °C. Brains were cut on a cryostat at −20 °C into 40-μm-thick coronal sections. Sections were

collected into antifreeze medium, and stored at −20 °C. After a thorough wash in 0.1 M phosphate-buffered saline (PBS) with 0.3% Triton X-100 (PBST), free-floating sections were incubated with 3% normal donkey serum (NDS) with 0.3% Triton X-100 for 20 min at room temperature. Sections were then incubated overnight at 4 °C with the primary antibody anti-$P2X_4R$ (1 : 400) in PBST–NDS solution. Slices were washed three times with 1 × PBS to rinse off the excess primary antibody before incubation for 2 h at room temperature with Alexa 488 goat anti-rabbit (Synaptic Systems, Göttingen, Germany) at 1 : 400 in PBST–NDS solution. After being washed three times with 1 × PBS, slices were fixed with fluoromont medium containing 4′,6-diamidino-2-phenylindole. Fluorescent images were acquired with a Leica DM6000 TCS SP8X microscope, with a diode laser (excitation – blue, 405 nm; white, 488 nm; and emission – green, 500–560 nm). Images were obtained by mosaic acquisition of the whole hippocampus at ×20.

Statistical analysis

Values are presented as mean ± standard error of the mean (SEM), and *n* indicates the number of different cells. For statistical analysis, non-parametric tests were used. Student's *t*-test was used for comparison between two groups, and one-way ANOVA followed by a Newman–Keuls *post hoc* test for comparison between more than two groups. Statistical differences were considered to be significant at $P < 0.05$. Note that, although the impacts of several drugs and modulators are presented as percentage values for the sake of clarity, statistical comparisons were always carried out with the absolute values. Statistical analysis was performed with PRISM 5.0 (GraphPad Software, La Jolla, CA, USA).

Results

LPS-treated microglia (LPS-microglia) increase basal synaptic transmission at MF–CA3 synapses

We first studied the effect of activated microglia on basal synaptic transmission. For this purpose, N9 microglia were first activated by pretreatment with LPS (100 ng/mL for 1 h) (Gomes *et al.*, 2013). Activated microglia were then added to acute hippocampal slices with previously described methodology (Centonze *et al.*, 2009). In our experimental condition, microglia fully covered the whole hippocampus and surrounded almost every CA3 pyramidal cell (Fig. 1A and B). Although microglia do not penetrate deeply into the slice, we recorded CA3 pyramidal cells surrounded (10–100 μm) by an average of three to five microglia in close vicinity, i.e. similar to the estimated density of microglia in the CA3 area (Jinno *et al.*, 2007). Consistent with previous observations (Centonze *et al.*, 2009), no noticeable differences in morphology between non-treated microglia (Fig. 1A) and LPS-microglia (Fig. 1B) were observed. However, we have not carried out detailed morphological analysis to determine whether the physical interaction between LPS-microglia and MF–CA3 synapses is similar to the interaction between endogenous microglia and MF–CA3 synapses.

To study basal synaptic transmission, MF-CA3 EPSCs (MF-EPSCs) were evoked with a minimal stimulation protocol (Marchal & Mulle, 2004). The average amplitude of MF-EPSCs recorded at a low stimulation rate (0.1 Hz) (−73 ± 5 pA; $n = 10$) was consistent with previous observations (Marchal & Mulle, 2004). The addition of non-treated microglia had no effect on basal synaptic transmission (−76 ± 12 pA; $P = 0.8$, $n = 9$) whereas the addition of LPS-microglia increased basal synaptic transmission (−106 ± 12 pA; $P < 0.05$, $n = 9$; data not shown) (Table 1).

LPS-microglia decrease short-term plasticity at MF-CA3 synapses

MF-CA3 synapses are distinct from most other synapses in the central nervous system, because they show prominent forms of presynaptic short-term plasticity (Nicoll & Schmitz, 2005), including pronounced paired-pulse facilitation (PPF) (two stimulations separated by 10–200 ms), represented by variation of the paired-pulse ratio (PPR) (pulse 2/pulse 1), and frequency facilitation (FF) (tonic stimulation switching from 0.1 Hz to >1 Hz). Activity-dependent neurotransmitter release among central nervous system synapses depends largely on the basal release probability, which is linked to the presynaptic calcium concentration. Hence, PPF at MF-CA3 synapses has been reported to depend solely on the residual calcium concentration in the presynaptic terminal (Salin *et al.*, 1996; Nicoll & Schmitz, 2005). MF-EPSCs recorded from slices with added LPS-microglia showed decreased PPF, estimated from the PPR, as compared with slices with no added microglia (LPS-microglia, 277 ± 31%; control, 392 ± 32%; $P < 0.05$, $n = 9$; Fig. 1C and E) and slices with non-treated microglia added (microglia, 357 ± 35%, $n = 9$; Fig. 1C and E). Added LPS-microglia also significantly decreased FF as compared with control (LPS-microglia, 281 ± 18%; control, 482 ± 39%; $P < 0.001$, $n = 9$; Fig. 1D and F) and slices with non-treated microglia added (microglia, 430 ± 18%; $P < 0.05$, $n = 9$; Fig. 1D and F). As both PPF and FF were similar between control slices and slices with added non-treated microglia, our results indicated that the decrease in short-term plasticity observed with added LPS-microglia was probably attributable to the immune challenging of microglia.

Inhibition of microglial A_{2A}Rs prevents changes in short-term plasticity

The immune challenging of microglia with LPS (100 ng/mL) is known to drive microglia to release ATP, and this is abolished by blocking adenosine A_{2A}Rs on microglia (Gomes *et al.*, 2013; George *et al.*, 2015). We thus hypothesized that ATP released from LPS-microglia was involved in the observed changes in short-term synaptic plasticity. Taking advantage of the fact that neuronal presynaptic A_{2A}Rs do not, as such, modulate basal synaptic transmission or either PPF or FF at MF synapses (Rebola *et al.*, 2008), we antagonized A_{2A}Rs on microglia by pre-incubation with the A_{2A}R antagonist SCH58261 (50 nM) for 20 min (Lopes *et al.*, 2004) prior to activation of microglia by LPS and addition to acute slices.

The pre-incubation of LPS-microglia with SCH58261 significantly reduced the decrease in FF induced by the addition of LPS-microglia (LPS-microglia, 281 ± 18%; LPS-microglia + SCH58261, 373 ± 27%; $P < 0.05$, $n = 9$) (Fig. 1F) but had no significant effect on the decrease in PPF (LPS-microglia, 277 ± 31%; LPS-microglia + SCH58261, 324 ± 31%; $P = 0.65$, $n = 9$) (Fig. 1E; Table 2). Thus, the blockade of A_{2A}Rs in LPS-microglia alleviated some of the changes observed in MF-CA3 short-term synaptic plasticity. As we have previously shown that A_{2A}Rs control ATP release from microglia (George *et al.*, 2015), this supports the hypothesis that ATP released from LPS-microglia might impact on MF-CA3 synaptic activity, leading to changes in short-term synaptic plasticity.

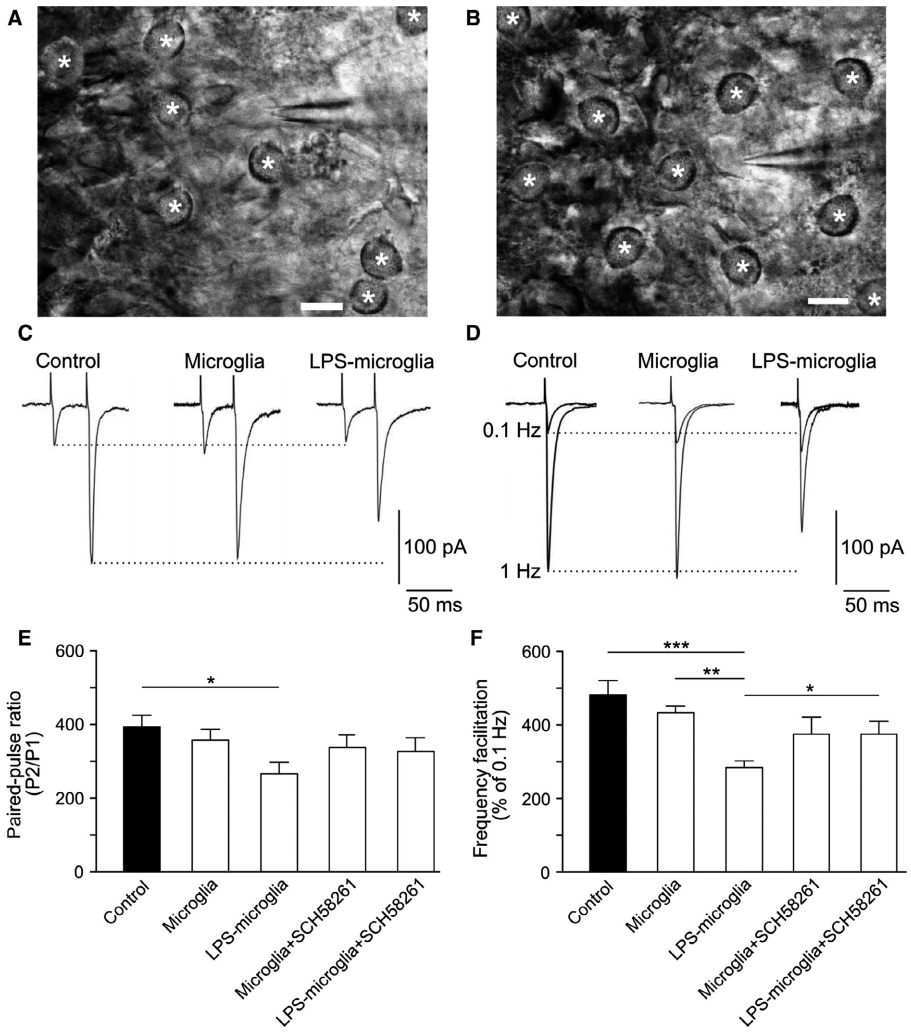

FIG. 1. LPS-microglia modulate short-term synaptic plasticity via a microglial $A_{2A}R$. (A) Non-treated microglia added to an acute hippocampal slice. A CA3 pyramidal cell was recorded in the whole cell configuration of the patch clamp technique, and is surrounded by microglia (*). Scale bar: 20 μm. (B) LPS-microglia (*) added to an acute hippocampal slice. Scale bar: 20 μm. (C) Representative traces of paired-pulse recordings obtained at 40 ms intervals, under different conditions. (D) Representative traces of EPSCs recorded at 0.1 Hz and 1 Hz, illustrating FF in different conditions. (E) Graphical representation of the PPR in different conditions. SCH58261 (50 nM) was added for 20 min prior to activation of microglia by LPS (control, 392 ± 32%; microglia, 357 ± 35%; LPS-microglia, 277 ± 31%; microglia + SCH58261, 336 ± 28%; LPS-microglia + SCH58261, 324 ± 31%; $n = 9$ for all conditions). (F) Graphical representation of FF in different conditions (control, 482 ± 39%; microglia, 430 ± 18%; LPS-microglia, 281 ± 18%; microglia + SCH58261, 375 ± 39%; LPS-microglia + SCH58261, 373 ± 27%; $n = 9$ for all conditions). FF and PPR protocols were performed one after another, on the same cell. Data are represented as mean ± SEM. *$P < 0.05$, **$P < 0.01$ and ***$P < 0.001$ from one-way ANOVA followed by a Newmann–Keuls multiple comparison test.

TABLE 1. Comparison of basal transmission (BT), PPF and FF with respect to control (slice alone)

Compared to control	Microglia	LPS-microglia	SCH58261-microglia	Apyrase	ARL67156	DPCPX	CCPA	5-BDBD	Ivermectin	$P2X_4$ KO
BT	–	↑	–	↓	–	↑	↓	↓	↑	↓
PPF	–	↓	–	–	–	–	–	↓	–	↓
FF	–	↓	–	–	↓	–	↓	–	↓	–

For each experimental condition, values are normalized to control. ↑, increase; ↓, decrease; –, no effect.

LPS-microglia regulate FF

To further validate the putative role of ATP, released by LPS-microglia, in the observed changes in FF and PPF, we manipulated extracellular ATP by either promoting its degradation with apyrase or by blocking its extracellular degradation with ARL67156 (Frenguelli *et al.*, 2007). Addition of apyrase (10 U/mL) decreased basal synaptic transmission at low frequency (0.1 Hz) within 5 min (control, 98 ± 1%; apyrase, 54 ± 1%; $P < 0.001$, $n = 4$) (Fig. 2A and B). In addition, apyrase abolished the decrease in FF induced by LPS-microglia (LPS-microglia, 281 ± 18%; LPS-microglia + apyrase, 393 ± 24%; $P < 0.01$, $n = 4$) (Fig. 2E). Apyrase also abolished the decrease in PPF induced by LPS-microglia (LPS-microglia, 277 ± 31%; LPS-microglia + apyrase, 466 ± 86%; $P < 0.05$, $n = 4$) (Fig. 2F). Conversely, ARL67156 was used in control slices

TABLE 2. Comparison of basal transmission (BT), PPF and FF with respect to LPS-microglia (slice + LPS-microglia)

Compared to LPS-microglia	SCH58261	Apyrase	DPCPX	CCPA	5-BDBD	$P2X_4$ KO
BT	↓	↓	↑	↓	↓	↓
PPF	–	↑	↑	–	–	↑
FF	↑	↑	–	–	↑	–

For each experimental condition, values are normalized to LPS-microglia. ↑, increase; ↓, decrease; –, no effect.

(no microglia added) to determine whether increasing the endogenous levels of ATP in control conditions could mimic the alterations induced by LPS-microglia. ARL67156 (100 μM) alone did not significantly affect the amplitude of MF-EPSCs recorded at 0.1 Hz (control, 98 ± 1%; ARL67156, 115 ± 13%; $P = 0.2$, $n = 4$) (Fig. 2C and D), but reduced FF as LPS-microglia did (control, 482 ± 39%; ARL67156, 183 ± 27%, $P < 0.001$; LPS-microglia, 281 ± 18%, $P < 0.001$, $n = 4$) (Fig. 2G). In contrast, ARL67156 did not significantly affect PPF (control, 392 ± 32%; ARL67156, 374 ± 71%; $P = 0.3$, $n = 3$) (Fig. 2H).

Hence, the decrease in FF induced by LPS-microglia was abolished by removal of extracellular ATP, whereas this decrease was mimicked by increased endogenous levels of ATP in control slices. In contrast, modulation of extracellular ATP did not have a significant effect on PPF; that is, manipulating the extracellular levels of ATP did not mimic or abolish the effects of LPS-microglia.

Adenosine is involved in LPS-microglia-mediated regulation of PPF

Our data strongly suggest that ATP is the key molecule responsible for the microglia-induced changes in presynaptic forms of short-term plasticity. However, ATP is readily converted into adenosine by extracellular ectonucleotidases (Cunha *et al.*, 1998), namely in synapses (Cunha, 2001), and presynaptic adenosine A_1Rs are present at MF–CA3 synapses (Scanziani *et al.*, 1992; Moore *et al.*, 2003; Kukley *et al.*, 2005; Rebola *et al.*, 2008). Therefore, we investigated whether adenosine derived from the ATP released by LPS-microglia could modulate MF–CA3 transmission.

We first studied the effects of CCPA (A_1R agonist) and of DPCPX [A_1R antagonist; see Sebastião *et al.* (2000)] on FF. As shown in Fig. 3B, DPCPX (100 nM) alone did not significantly change FF (control, 482 ± 39%; DPCPX, 426 ± 87%; $P = 0.5$, $n = 9$), in agreement with previous studies (Kukley *et al.*, 2005; Rebola *et al.*, 2008) [but see Moore *et al.* (2003)], and also had no effect on basal synaptic transmission (control, 147 ± 18%; DPCPX, 97 ± 3%; $P = 0.06$, $n = 9$; data not shown). DPCPX did not abolish the LPS-microglia-induced decrease in FF (LPS-microglia, 281 ± 18%; LPS-microglia + DPCPX, 250 ± 38%; $P = 0.8$, $n = 9$) (Fig. 3B). Furthermore, CCPA (100 nM) did not mimic the effect of LPS-microglia on FF (CCPA, 399 ± 52%; LPS-microglia, 281 ± 18%; $P = 0.08$, $n = 9$) (Fig. 3D). Finally, CCPA did not alter the LPS-microglia-induced decrease in FF (LPS-microglia, 281 ± 18%; LPS-microglia + CCPA, 230 ± 42%; $P = 0.2$, $n = 9$) (Fig. 3D). In contrast, DPCPX prevented the change in PPF induced by LPS-microglia (LPS-microglia, 277 ± 31%; LPS-microglia + DPCPX, 383 ± 35%, $P > 0.05$, $n = 9$) (Fig. 3C). Conversely, CCPA decreased PPF when added to control slices (control, 392 ± 32%; CCPA, 269 ± 38%; $P > 0.05$, $n = 9$) (Fig. 3E), mimicking the effect of LPS-microglia.

Taken together, these results indicate that the level of extracellular adenosine in our experimental conditions was moderate, as estimated by the lack of a significant effect of DPCPX on basal synaptic transmission, and show that, whereas adenosine produced by the breakdown of released ATP from LPS-microglia has no effect on FF, it modulates PPF.

$P2X_4$Rs modulate short-term synaptic plasticity

To further characterize the role of ATP derived from LPS-microglia in the modulation of FF, we investigated which subtype of purinergic receptor was involved. ATP can bind to metabotropic (P2Y) and ionotropic (P2X) receptors. A role of P2X receptors has been reported in hippocampal synapses, mostly in the context of synaptic plasticity (Soto *et al.*, 1996; Khakh *et al.*, 1999; Pankratov *et al.*, 2002; Priel & Silberberg, 2004; Sim *et al.*, 2006; Pougnet *et al.*, 2014). As shown in Fig. 4A, the effect of LPS-microglia on FF was prevented by blocking P2X receptors with the broad-spectrum antagonist PPADS (50 μM) (Lambrecht *et al.*, 2002) (LPS-microglia, 281 ± 18%; LPS-microglia + PPADS, 427 ± 56%; $P > 0.05$, $n = 9$). In contrast, PPADS had no effect on the decrease in PPF induced by LPS-microglia (LPS-microglia, 277 ± 31%; LPS-microglia + PPADS, 281 ± 22%; $P = 0.9$, $n = 9$) (Fig. 4B). These results provide evidence that P2X receptors specifically modulated FF, and not PPF.

We next investigated which subtype of P2X receptor was responsible for the effect of LPS-microglia on FF. The presynaptic expression of $P2X_7$Rs at MFs remains controversial (Armstrong *et al.*, 2002; Sperlágh *et al.*, 2002; Kukley *et al.*, 2004; Yu *et al.*, 2008), whereas the involvement of $P2X_4$Rs in the modulation of synaptic strength (Baxter *et al.*, 2011) and/or plasticity has been documented (Sim *et al.*, 2006) at CA3–CA1 synapses. However, the presence of $P2X_4$Rs at MF synapses remains to be studied. We first investigated whether $P2X_4$Rs were involved in the modulation of basal synaptic transmission. Application of the selective $P2X_4$R antagonist 5-BDBD (10 μM) (Donnelly-Roberts *et al.*, 2008) decreased basal synaptic transmission at low frequency (0.1 Hz) within 5 min of its addition (control, 98 ± 1%; 5-BDBD, 65 ± 4%; $P < 0.001$, $n = 9$) (Fig. 4C and D). Conversely, ivermectin (3 μM), a positive allosteric modulator of $P2X_4$Rs that potentiates $P2X_4$R currents (Khakh *et al.*, 1999; Sim *et al.*, 2006), increased basal synaptic transmission at low frequency (0.1 Hz) within 10 min of its addition (control, 98 ± 1%; ivermectin, 128 ± 7%; $P < 0.05$, $n = 6$) (Fig. 4E and F). Consistent with these results, basal synaptic transmission was also decreased in slices obtained from $P2X_4$R knockout (KO) mice (control, 98 ± 1%; $P2X_4$R KO, 85 ± 6%; $P < 0.05$, $n = 9$; data not shown). Therefore, ATP modulates basal synaptic transmission at MF-CA3 synapses through $P2X_4$Rs.

We then investigated the putative role of $P2X_4$Rs in the modulation of FF. Selective blockade of $P2X_4$Rs with 5-BDBD on its own had no effect on FF (control, 482 ± 39%; 5-BDBD, 438 ± 25%; $P = 0.12$, $n = 9$), whereas potentiation of $P2X_4$Rs by ivermectin significantly decreased FF (control, 482 ± 39%; ivermectin, 344 ± 35%; $P < 0.05$, $n = 9$) (Fig. 4G). Conversely, 5-BDBD on its own decreased PPF (control, 392 ± 32%; 5-BDBD, 227 ± 16%; $P < 0.01$, $n = 9$), whereas ivermectin had no effect (control, 392 ± 32%; ivermectin, 369 ± 40%; $P = 0.66$, $n = 9$) (Fig. 4H).

These results provide good evidence that activation of $P2X_4$Rs modulates FF but not PPF, and suggest a presynaptic site of action for ATP. To further strengthen the hypothesis of presynaptic localization of $P2X_4$Rs, we used a new antibody raised against $P2X_4$Rs and checked its specificity in slices from $P2X_4$R KO mice. As

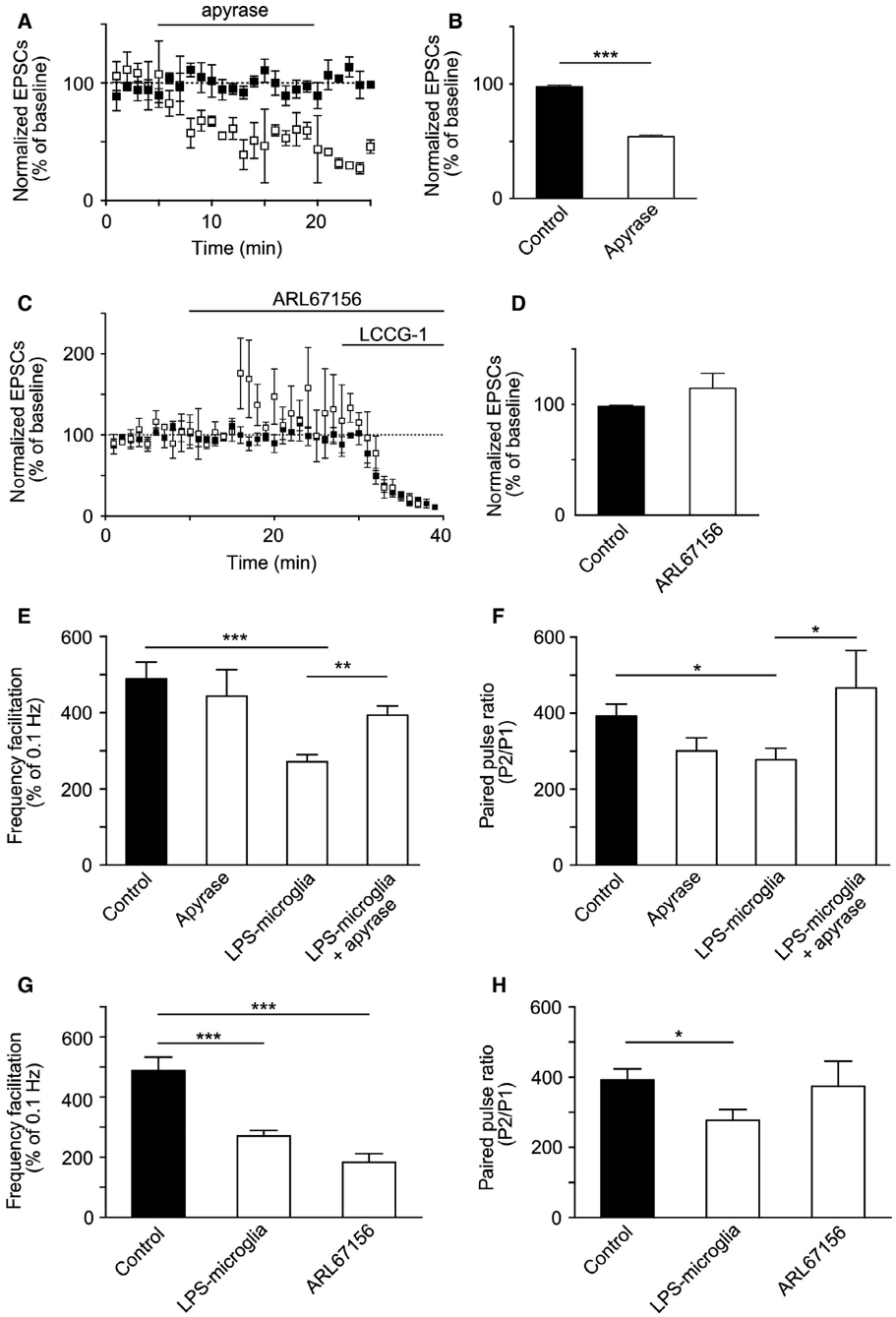

FIG. 2. LPS-microglia-derived ATP modulates synaptic transmission and short-term plasticity. (A) Summary plot of the effect of apyrase on basal synaptic transmission recorded at low frequency of stimulation (0.1 Hz). Apyrase (10 U/mL) induced a decrease in basal synaptic transmission as measured by the amplitude of EPSCs (control, black squares; apyrase, open squares). (B) Graphical representation of the basal synaptic transmission shown in A (control, 98 ± 1%, $n = 9$; apyrase, 54 ± 1%, $n = 4$). (C) Summary plot of the effect of ARL67156 (100 μM) on basal synaptic transmission recorded at low frequency of stimulation (0.1 Hz). ARL67156 did not significantly affect the amplitude of MF-EPSCs within 10 min of addition ($n = 4$) (control, black squares; ARL67156, open squares). LCCG-1 (10 μM), a metabotropic glutamate receptor 2 agonist, was added to confirm the selective stimulation of MFs. (D) Graphical representation of the basal synaptic transmission shown in C (control, 98 ± 1%, $n = 9$; ARL67156, 115 ± 13%, $n = 4$). (E) Graphical representation of FF. Apyrase abolished the effect of LPS-microglia on FF (control, 482 ± 39%, $n = 9$; apyrase, 444 ± 69%, $n = 4$; LPS-microglia, 281 ± 18%, $n = 9$; LPS-microglia + apyrase, 393 ± 24%, $n = 4$). (F) Graphical representation of PPR. Apyrase abolished the reduction in PPR induced by LPS-microglia (control, 392 ± 32%, $n = 9$; apyrase, 301 ± 34%, $n = 4$; LPS-microglia, 277 ± 31%, $n = 9$; LPS-microglia + apyrase, 466 ± 86%, $n = 4$). (G) Graphical representation of FF. Addition of ARL67156 (100 μM) mimicked the LPS-microglia-induced decrease in FF (control, 482 ± 39%, $n = 9$; LPS-microglia, 281 ± 18%, $n = 9$; ARL67156, 183 ± 27%, $n = 3$). (H) Graphical representation of PPR. Increasing the extracellular level of ATP with ARL67156 (100 μM) had no effect on PPR (control, 392 ± 32%, $n = 9$; LPS-microglia, 277 ± 31%, $n = 9$; ARL67156, 374 ± 71%, $n = 3$). Values in all graphs are mean ± SEM. $^*P < 0.05$, $^{**}P < 0.01$ and $^{***}P < 0.001$ from one-way ANOVA followed by a Newmann–Keuls multiple comparison test.

shown in Fig. 4I, we observed strong immunostaining for $P2X_4R$ (green) on the MF tract (upper panel) that was almost completely absent in slices from $P2X_4R$ KO mice (lower panel). It is worth noting that we did not observe clear $P2X_4R$ immunoreactivity in the CA1 area, in contrast to previous reports (Rubio & Soto, 2001; Sim *et al.*, 2006), suggesting the possibility that different antibodies may

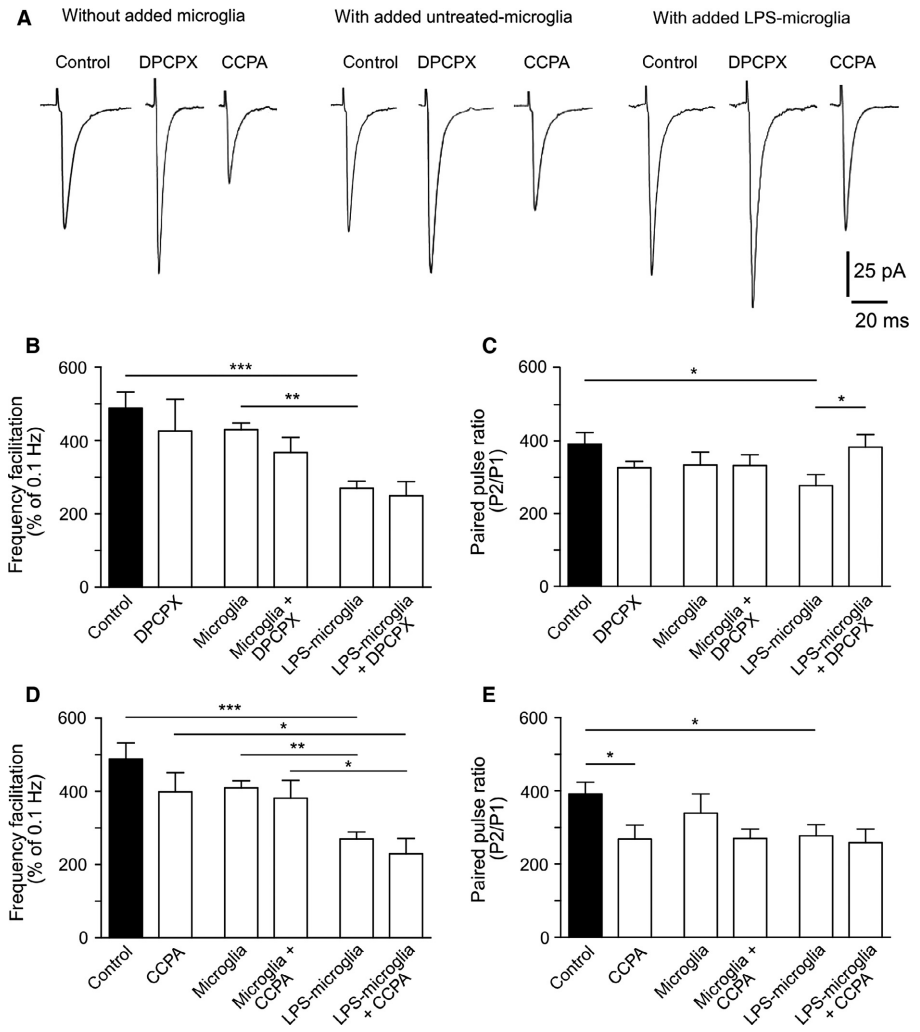

FIG. 3. LPS-microglia-induced modulation of PPF involves adenosine and presynaptic A_1Rs. (A) Representative traces of EPSCs triggered at a low frequency of stimulation (0.1 Hz). (B) Graphical representation of FF. Blockade of A_1Rs by DPCPX (100 nM) had no effect on the LPS-microglia-induced change in FF (control, 482 ± 39%; DPCPX, 426 ± 87%; microglia, 430 ± 18%; microglia + DPCPX, 367 ± 41%; LPS-microglia, 281 ± 18%; LPS-microglia + DPCPX, 250 ± 38%; $n = 9$ for all conditions). (C) Graphical representation of the PPR. Blockade of A_1Rs inhibited the reduction in the PPR induced by LPS-microglia (control, 392 ± 32%; DPCPX, 326 ± 18%; microglia, 357 ± 35%; microglia + DPCPX, 333 ± 29%; LPS-microglia, 277 ± 31%; LPS-microglia + DPCPX, 383 ± 35%; $n = 9$ for all conditions). (D) Graphical representation of FF. CCPA (100 nM) did not alter the LPS-microglia-induced decrease in FF (control, 482 ± 39%; CCPA, 399 ± 52%; microglia, 430 ± 18%; microglia + CCPA, 382 ± 48%; LPS-microglia, 281 ± 18%; LPS-microglia + CCPA, 230 ± 42%; $n = 9$ for all conditions). (E) Graphical representation of the PPR. CCPA decreased the PPR, mimicking the effect of LPS-microglia (control, 392 ± 32%; CCPA, 269 ± 38%; microglia, 357 ± 35%; microglia + CCPA, 270 ± 25%; LPS-microglia, 277 ± 31%; LPS-microglia + CCPA, 259 ± 37%; $n = 9$ for all conditions). Values in all graphs are mean ± SEM. $^*P < 0.05$, $^{**}P < 0.01$ and $^{***}P < 0.001$ from one-way ANOVA followed by a Newmann–Keuls multiple comparison test.

recognize different known molecular structures of homomeric $P2X_4$Rs (Zemkova *et al.*, 2015), different known heteromeric receptor complexes containing $P2X_4$R subunits (Antonio *et al.*, 2014), or $P2X_4$Rs with different subcellular localizations (Xu *et al.*, 2014).

$P2X_4$Rs mediate the LPS-microglia-induced decrease in FF

We then investigated the possible involvement of $P2X_4$Rs in the modulation of FF by LPS-microglia. Blockade of $P2X_4$Rs in hippocampal slices before the addition of LPS-microglia prevented the decrease in FF (LPS-microglia + 5-BDBD, 378 ± 28%; LPS-microglia, 281 ± 18%; $P < 0.01$, $n = 9$) (Fig. 5B) but did not alleviate the decrease in PPF (LPS-microglia + 5-BDBD, 242 ± 25%; LPS-microglia, 277 ± 31%; $P = 0.09$, $n = 9$) (Fig. 5C). Because $P2X_4$Rs are also dynamically involved in controlling endogenous microglia (Toulme & Khakh, 2012; Koizumi *et al.*, 2013) as well as N9 microglia (Xiang & Burnstock, 2005), we investigated whether the effect of 5-BDBD was attributable to $P2X_4$Rs expressed at MF-CA3 synapses or those expressed by N9 microglia added to the slice. For this purpose, LPS-microglia were added to hippocampal slices obtained from $P2X_4$R KO mice.

The decrease in FF induced by LPS-microglia was reduced in slices obtained from $P2X_4$R KO mice (LPS-microglia + $P2X_4$R KO, 337 ± 23%; LPS-microglia, 281 ± 18%; $P < 0.05$, $n = 6$) (Fig. 5D), whereas the decrease in PPF induced by LPS-microglia was preserved in slices from $P2X_4$R KO mice (LPS-microglia + $P2X_4$R KO, 265 ± 41%; LPS-microglia, 277 ± 31%; $P = 0.8$, $n = 9$) (Fig. 5E).

The ectonucleotidase inhibitor ARL67156 (10 μM) mimicked the LPS-microglia-induced decrease in FF (control, 482 ± 39%, $n = 9$;

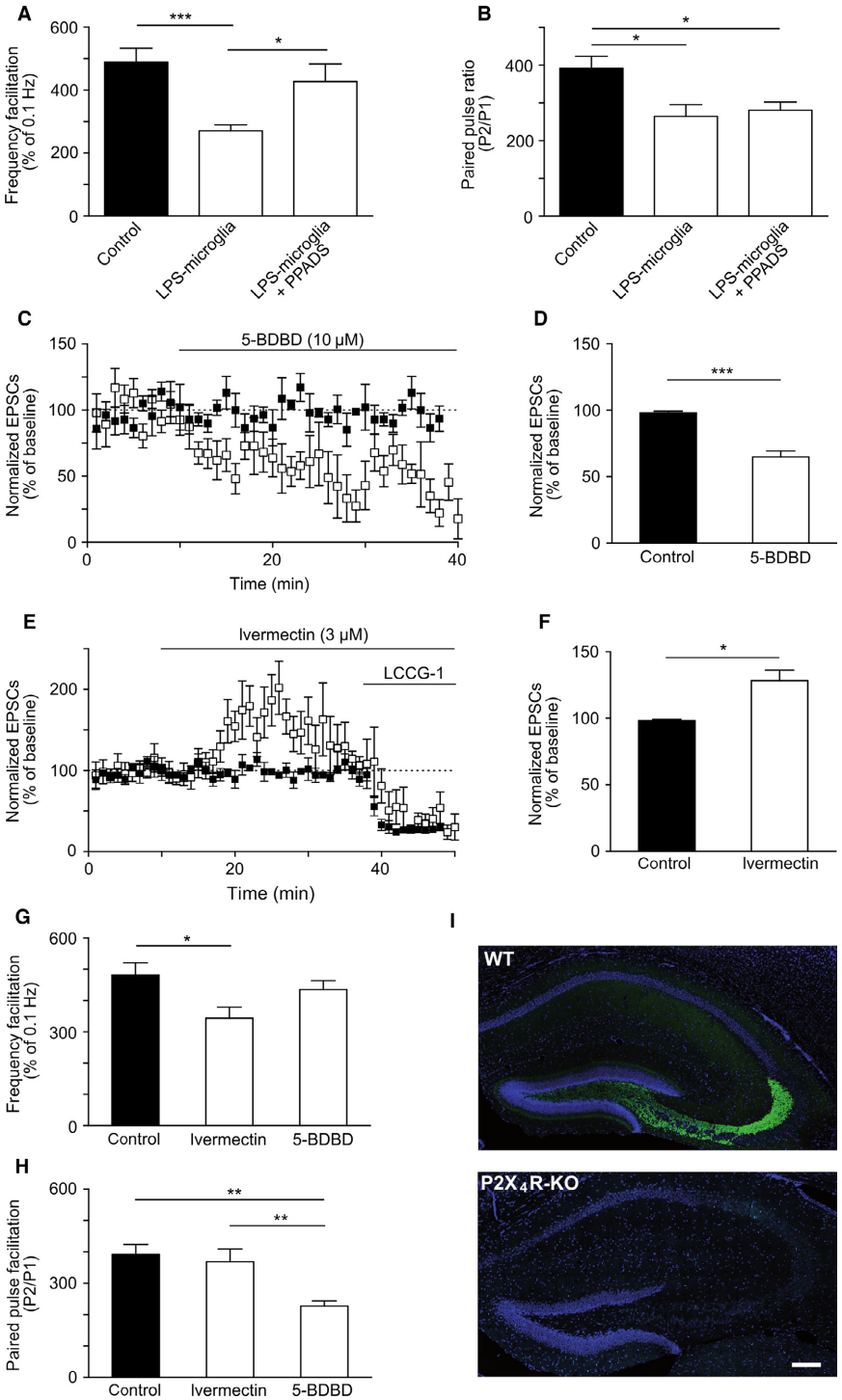

FIG. 4. Extracellular ATP modulates basal synaptic transmission and FF via presynaptic $P2X_4Rs$. (A) Graphical representation of FF. PPADS (50 μM) blocked the LPS-microglia-induced decrease in FF (control, 482 ± 39%; LPS-microglia, 281 ± 18%; LPS-microglia + PPADS, 427 ± 56%; $n = 9$ for all conditions). (B) Graphical representation of PPR. PPADS (50 μM) had no effect on the LPS-microglia-induced decrease in PPR (control, 392 ± 32%; LPS-microglia, 277 ± 31%; LPS-microglia + PPADS, 281 ± 22%; $P = 0.9$, $n = 9$ for all conditions). (C) Summary plot of the effect of 5-BDBD (10 μM) on basal synaptic transmission. 5-BDBD induced a decrease in basal synaptic transmission within 5 min of addition (control, black squares; 5-BDBD, open squares). (D) Graphical representation of the basal synaptic transmission shown in C (control, 98 ± 1%; 5-BDBD, 65 ± 4%; $n = 9$ for both conditions). (E) Summary plot of the effect of ivermectin (3 μM) on basal synaptic transmission. Ivermectin increased basal synaptic transmission within 10 min of addition (control, black squares; ivermectin, open squares). (F) Graphical representation of the basal synaptic transmission shown in E (control, 98 ± 1%, $n = 9$; ivermectin, 128 ± 7%, $n = 6$). The values in A, B, D and F are mean ± SEM; $*P < 0.05$ and $***P < 0.001$, unpaired t-test. (G) Graphical representation of FF. Ivermectin (3 μM) decreased FF, whereas 5-BDBD (10 μM) had no effect (control, 482 ± 39%, $n = 9$; ivermectin, 344 ± 35%, $n = 6$; 5-BDBD, 438 ± 25%, $n = 9$). (H) Graphical representation of PPR. 5-BDBD (10 μM) decreased PPR, whereas ivermectin (3 μM) had no effect (control, 392 ± 32%, $n = 9$; ivermectin, 369 ± 40%, $n = 6$; 5-BDBD, 227 ± 16%, $n = 9$). The values in G and H are mean ± SEM; $*P < 0.05$ and $**P < 0.01$ from one-way ANOVA followed by a Newmann–Keuls multiple comparison test. (I) The hippocampal MFs showed strong immunostaining for $P2X_4R$ (green) in a wild-type (WT) mouse (upper panel), whereas it was virtually absent in a slice from a $P2X_4R$ KO mouse (lower panel). 4′,6-Diamidino-2-phenylindole staining for nuclei is shown in blue. Scale bar: 200 μm.

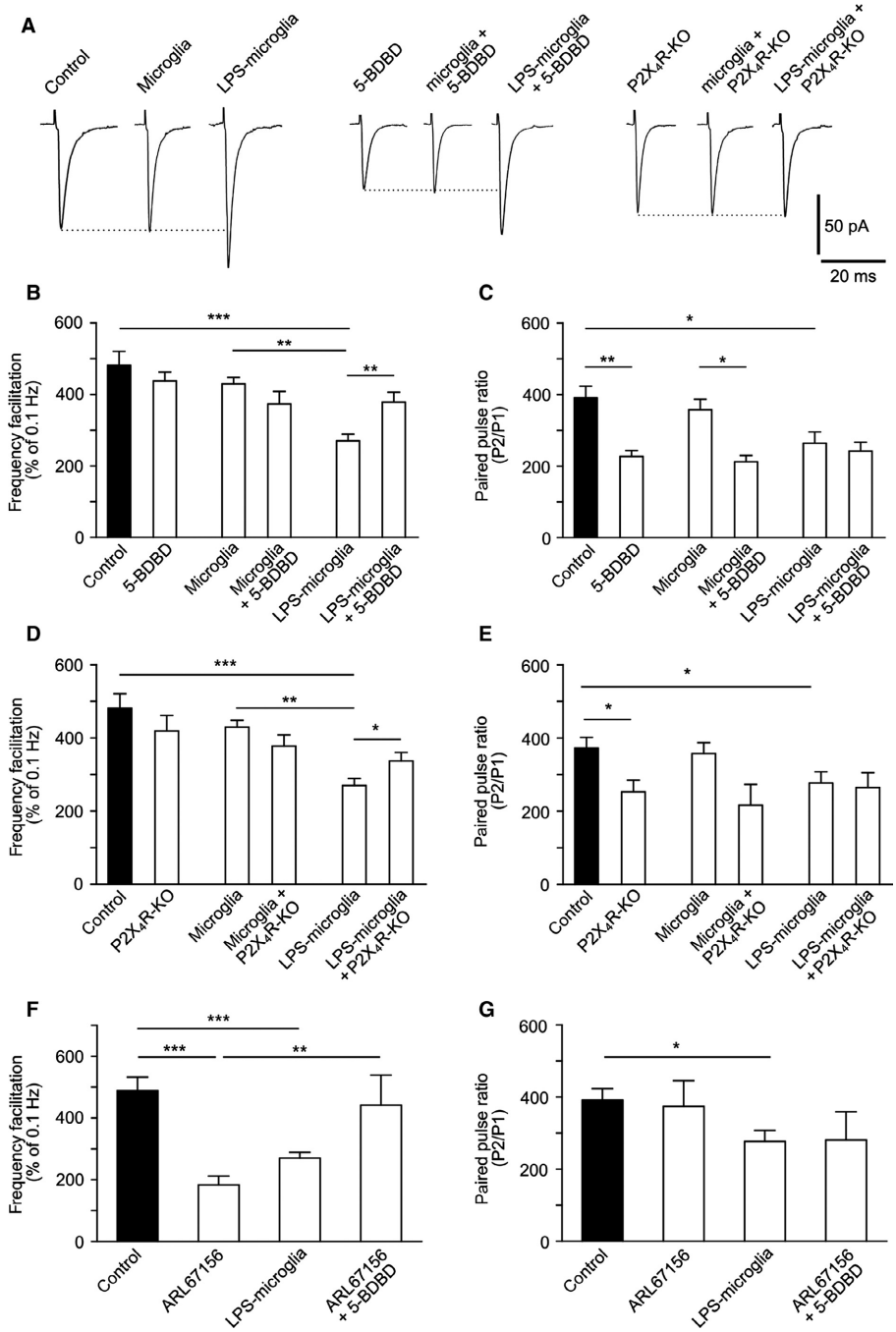

FIG. 5. LPS-microglia-derived ATP regulates FF via $P2X_4Rs$. (A) Representative traces of EPSCs triggered at low frequency of stimulation (0.1 Hz). (B) Graphical representation of FF. Blockade of $P2X_4Rs$ by 5-BDBD (10 μM) inhibited the effect of LPS-microglia on FF (control, 482 ± 39%; 5-BDBD, 438 ± 25%; microglia, 430 ± 18%; microglia + 5-BDBD, 374 ± 35%; LPS-microglia, 281 ± 18%; LPS-microglia + 5-BDBD, 378 ± 28%; $n = 9$ for all conditions). (C) Graphical representation of the PPR. 5-BDBD (10 μM) had no effect on the decrease in the PPR induced by LPS-microglia, whereas it reduced it when applied alone (control, 392 ± 32%; 5-BDBD, 227 ± 16%; microglia, 357 ± 35%; microglia + 5-BDBD, 212 ± 18%; LPS-microglia, 277 ± 31%; LPS-microglia + 5-BDBD, 242 ± 25%; $n = 9$ for all conditions). (D) Bar representation of FF. Genetic deletion of $P2X_4R$ ($P2X_4R$ KO) abolished the LPS-microglia induced decrease in FF (control, 482 ± 39%; $P2X_4R$ KO, 419 ± 43%; microglia, 430 ± 18%; microglia + $P2X_4R$ KO, 377 ± 31%; LPS-microglia, 281 ± 18%; LPS-microglia + $P2X_4R$ KO, 337 ± 23%; $n = 9$ for all conditions). (E) Graphical representation of the PPR. The LPS-microglia-induced decrease in the PPR was preserved in $P2X_4R$ KO slices (control, 392 ± 32%; $P2X_4R$ KO, 253 ± 32%; microglia, 357 ± 35%; microglia + $P2X_4R$ KO, 216 ± 57%; LPS-microglia, 277 ± 31%; LPS-microglia + $P2X_4R$ KO, 265 ± 41%; $n = 9$ for all conditions). (F) Graphical representation of FF. Addition of ARL67156 (10 μM) mimicked the LPS-microglia-induced decrease in FF, whereas prior blockade of $P2X_4Rs$ by 5-BDBD (10 μM) prevented this effect (control, 482 ± 39%, $n = 9$; ARL67156, 183 ± 29%, $n = 3$; LPS-microglia, 281 ± 18%, $n = 9$; ARL67156 + 5-BDBD, 442 ± 97%, $n = 3$). (G) Graphical representation of the PPR. Increasing the level of endogenous ATP with ARL67156 (10 μM) had no effect on the PPR (control, 392 ± 32%, $n = 9$; ARL67156, 324 ± 71%, $n = 3$; LPS-microglia, 277 ± 31%, $n = 9$; ARL67156 + 5-BDBD, 281 ± 78%, $n = 3$). Values in all graphs are mean ± SEM. $^*P < 0.05$, $^{**}P < 0.01$ and $^{***}P < 0.001$ from one-way ANOVA followed by a Newmann–Keuls multiple comparison test.

LPS-microglia, 281 ± 18%; $P < 0.001$, $n = 9$; ARL67156, 183 ± 29%; $P < 0.001$, $n = 3$) (Fig. 5F), whereas prior blockade of $P2X_4$Rs by 5-BDBD (10 μM) prevented this effect (ARL67156 + 5-BDBD, 442 ± 97%; $P < 0.02$, $n = 3$) (Fig. 5F). In contrast, prior blockade of $P2X_4$Rs by 5-BDBD, before addition of ARL67156, had no further effect on PPF (Fig. 5G).

ATP and adenosine modulate synaptic plasticity independently of each other

Our data strongly suggest that extracellular ATP released from LPS-microglia acts on $P2X_4$Rs to modulate FF, and that adenosine catabolized from extracellular ATP acts on A_1Rs to modulate PPF. Adenosine being the end-product of ATP, we had to disentangle any possible indirect effects of ATP on PPF or adenosine on FF. For this purpose, FF and PPF were investigated in the presence of DPCPX in slices obtained from $P2X_4$R KO mice. The LPS-microglia-induced decrease in FF (Fig. 6A and B) was reduced in $P2X_4$R KO mice (LPS-microglia, 281 ± 18%; LPS-microglia + $P2X_4$R KO, 337 ± 23%; $P < 0.05$, $n = 9$), but was preserved in the presence of DPCPX (LPS-microglia + $P2X_4$R KO + DPCPX, 402 ± 38%; $P < 0.001$, $n = 5$) (Fig. 6B). This indicates that A_1Rs have no effect on the modulation of FF by $P2X_4$Rs. Conversely, genetic deletion of $P2X_4$Rs did not prevent the ability of DPCPX to block the LPS-microglia-induced decrease in PPF (Fig. 6C and D). Hence, ATP released by LPS-microglia and its end-product adenosine act independently on $P2X_4$Rs and A_1Rs, respectively, to modulate short-term synaptic plasticity.

Discussion

Over the last 10 years, the notion of microglia as passive sentinels within the brain has been noticeably widened, and microglia are now acknowledged to constitute a new partner in synaptic function (Tremblay *et al.*, 2010) [reviewed in Kettenmann *et al.* (2013)]. Indeed, microglia can secrete a full array of neuroactive molecules, including several proinflammatory cytokines (interleukin-1β, interleukin-6, and tumour necrosis factor-α), trophic factors such as brain-derived neurotrophic factor, and also neurotransmitters such as ATP, glycine, and glutamate [reviewed in Kettenmann *et al.* (2011)]. In the present study, we focused on the putative effect of microglia-derived purines on synaptic function at MF-CA3 synapses. In this experimental paradigm, N9 microglia were previously challenged with an immune stimulus (LPS) to induce them to release ATP (George *et al.*, 2015), and were then added to hippocampal slices.

Combining pharmacological, electrophysiological and immunohistochemical approaches, our study demonstrated that ATP released

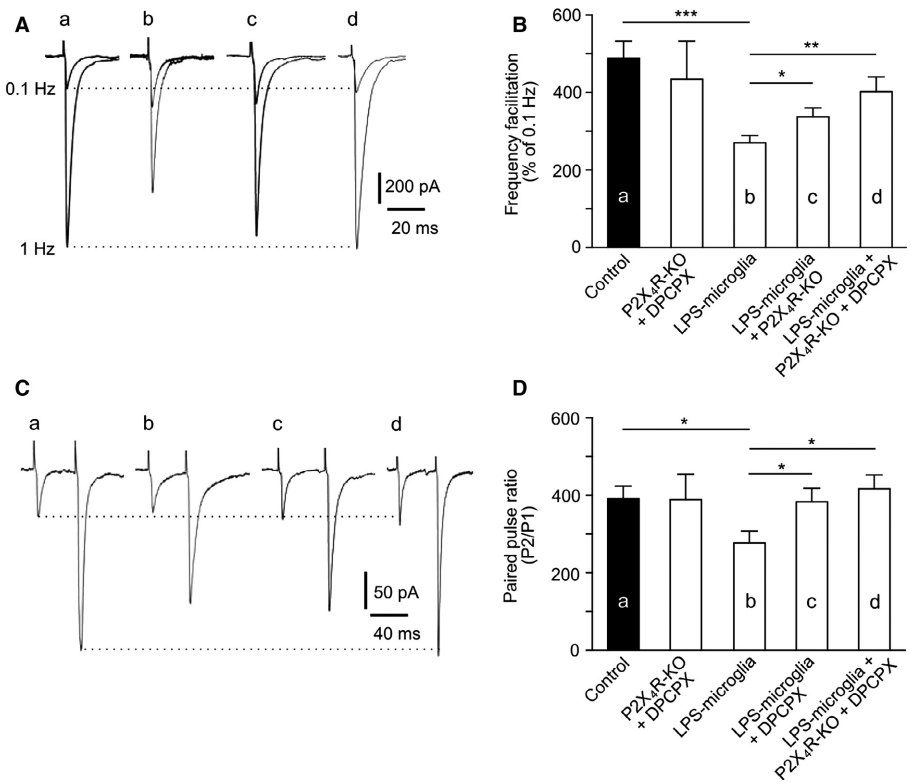

FIG. 6. ATP and adenosine act independently on $P2X_4$Rs and A_1Rs. (A) Representative traces of EPSCs recorded at 0.1 Hz and 1 Hz, illustrating FF in different conditions. (a) Control. (b) LPS-microglia. (c) LPS-microglia + $P2X_4$R KO. (d) LPS-microglia + $P2X_4$R KO + DPCPX. (B) Graphical representation of FF. Blockade of A_1R by DPCPX (100 nM) had no effect on the inhibitory effect of $P2X_4$R KO on the LPS-microglia-induced change in FF (control, 482 ± 39%, $n = 9$; $P2X_4$R KO + DPCPX, 434 ± 98%, $n = 5$; LPS-microglia, 281 ± 18%, $n = 9$; LPS-microglia + $P2X_4$R KO, 337 ± 23%, $n = 9$; LPS-microglia + $P2X_4$R KO + DPCPX, 402 ± 38%, $n = 5$). (C) Representative traces of EPSCs recorded at 0.1 Hz, illustrating the PPR in different conditions. (a) Control. (b) LPS-microglia. (c) LPS-microglia + DPCPX. (d) LPS-microglia + $P2X_4$R KO + DPCPX. (D) Graphical representation of the PPR. Genetic deletion of $P2X_4$Rs had no effect on the DPCPX-induced inhibition of the LPS-microglia-induced decrease in the PPR (control, 392 ± 32%, $n = 9$; $P2X_4$R KO + DPCPX, 388 ± 66%, $n = 5$; LPS-microglia, 277 ± 31%, $n = 9$; LPS-microglia + DPCPX, 383 ± 35%, $n = 9$; LPS-microglia + $P2X_4$R KO + DPCPX, 417 ± 36%, $n = 5$). Values in all graphs are mean ± SEM. $^*P < 0.05$, $^{**}P < 0.01$ and $^{***}P < 0.001$ from one-way ANOVA followed by a Neumann–Keuls multiple comparison test.

by LPS-microglia modulates MF-CA3 synaptic transmission both directly via presynaptic $P2X_4Rs$ and through its metabolite adenosine, by acting on presynaptic A_1Rs. Each pathway selectively modulates a different type of short-term presynaptic plasticity at MF-CA3 synapses, namely FF for $P2X_4Rs$ and PPF for A_1Rs. This study reveals complex crosstalk between microglial release of ATP, purinergic receptor activation, and hippocampal synaptic function.

$P2X_4Rs$ modulate basal synaptic transmission

Basal synaptic transmission at MF-CA3 synapses is governed by presynaptic intracellular calcium homeostasis and cAMP levels (Nicoll & Schmitz, 2005). Within the ionotropic P2X receptor family, $P2X_4Rs$ show the highest permeability for calcium (Soto *et al.*, 1996; Burnstock *et al.*, 2011), and, through this property, $P2X_4Rs$ can modulate basal synaptic transmission. In good agreement with this, the blockade of $P2X_4Rs$ by 5-BDBD or their genetic deletion in $P2X_4R$ KO mice decreased basal synaptic transmission, whereas ivermectin, which selectively potentiates ATP-induced currents at $P2X_4Rs$ (Khakh *et al.*, 1999; Priel & Silberberg, 2004), increased it. As expected, the degradation of extracellular ATP by apyrase also decreased basal synaptic transmission. All together, these results suggest that extracellular ATP tonically modulates basal synaptic transmission, most likely by increasing the presynaptic calcium concentration via its influx through $P2X_4Rs$.

Interestingly, the end-product of ATP catabolism, i.e. adenosine, by acting on presynaptic A_1Rs, also tonically decreases basal synaptic transmission (Moore *et al.*, 2003; Kukley *et al.*, 2005; Rebola *et al.*, 2008), probably through the direct A_1R inhibition of calcium influx via presynaptic P/Q-type and N-type calcium channels (Gundlfinger *et al.*, 2007). Our results suggest that purines modulate basal synaptic transmission via a complex interplay between ATP and adenosine signalling, which produce opposite effects.

Microglia-derived ATP impacts on FF

Owing to their unusual low initial glutamate release probability, MF-CA3 synapses show a large facilitation of response amplitudes of up to 500–600% when the frequency of stimulation is increased from 0.1 Hz to 1 Hz. This unique form of short-term plasticity, termed FF, was decreased by 40–50% following the addition of LPS-microglia. Several lines of evidence clearly demonstrate that ATP produced by LPS-microglia and acting on $P2X_4Rs$ was responsible for this effect: first, the addition of unstimulated microglia to acute slices had no effect on FF; second, the decrease in FF following the addition of LPS-microglia was prevented by apyrase but potentiated by ARL67156; third, it was blocked by PPADS, a broad-spectrum P2X receptor antagonist, but also by 5-BDBD; fourth, it was mimicked by ivermectin; fifth, it was absent in $P2X_4R$ KO mice; and sixth, it was insensitive to the A_1R ligands DPCPX (antagonist) and CCPA (agonist), in agreement with previous work (Rebola *et al.*, 2008).

It is not known for certain how FF is governed at MF-CA3 synapses, and different mechanisms have been proposed, such as the involvement of calcium/calmodulin-dependent protein kinase II (Salin *et al.*, 1996), presynaptic kainate receptors (Contractor *et al.*, 2001), or presynaptic voltage-dependent calcium channels (Gundlfinger *et al.*, 2007). Our results show that $P2X_4Rs$ only control FF in the presence of sufficient amounts of extracellular ATP, which are probably provided by activated microglia, whereas, in the absence of LPS-microglia, FF is insensitive to $P2X_4R$ blockade.

Microglia-derived adenosine but not ATP impacts on PPF

The decrease in PPF induced by LPS-microglia, which was preserved in the presence of PPADS or 5-BDBD but also in $P2X_4R$ KO slices, strongly suggests that adenosine but not ATP was involved in this effect. Activation of A_1Rs at MF-CA3 synapses is known to inhibit synaptic transmission (Scanziani *et al.*, 1992; Moore *et al.*, 2003; Kukley *et al.*, 2005), and its presynaptic localization has been confirmed by electron microscopy (Rebola *et al.*, 2008). The blockade by DPCPX of the decrease in PPF induced by LPS-microglia and its mimicking by CCPA are good evidence that adenosine resulting from the degradation of microglia-derived ATP modulates PPF. Unexpectedly, the blockade of $P2X_4Rs$ by 5-BDBD on its own also reduced PPF. This could indicate that endogenous ATP in the presence of receptors blocked by 5-BDBD would be more readily available to be converted into adenosine, activating A_1R and leading to a decrease in PPF. Hence, PPF was not affected in $P2X_4R$ KO mice, supporting our contention that the effect of 5-BDBD involves greater availability of adenosine acting on A_1Rs rather than an effect of $P2X_4R$.

Owing to a very low initial release probability, the PPF at MF-CA3 synapses is assumed to be directly linked to the probability of glutamate release, which is dependent on the residual calcium concentration in the presynaptic terminal (Salin *et al.*, 1996; Nicoll & Schmitz, 2005). Therefore, one could expect that microglia-derived adenosine acting on A_1Rs by reducing calcium influx into MF terminals (Gundlfinger *et al.*, 2007) would decrease PPF instead of increasing it. However, conflicting results have been reported for the impact of A_1R activation on PPF at MF-CA3 synapses, ranging from a reduction by half of PPF by DPCPX (Moore *et al.*, 2003) to no effect at all (Kukley *et al.*, 2005). These opposite results were attributed to differences in the ambient levels of adenosine in slices. Our results are consistent with a moderate level of ambient adenosine, as shown by the weak increase in basal synaptic transmission caused by DPCPX, similarly to what was previously reported (Kukley *et al.*, 2005; Rebola *et al.*, 2008), and by the lack of a significant effect on PPF.

Pathophysiological relevance of microglia-derived purine modulation of MF-CA3 synaptic plasticity

There is compelling evidence that the purinergic system is instrumental in neuroinflammation (Di Virgilio *et al.*, 2009), which can impact on synaptic function (Ben Achour & Pascual, 2010; Pascual *et al.*, 2012). ATP is a major trigger of microglia activation through $P2X_4Rs$ and $P2X_7$ receptors (Di Virgilio *et al.*, 2009; Koizumi *et al.*, 2013), and adenosine also regulates microglia responses through the activation of $A_{2A}Rs$ *in vivo* (Rebola *et al.*, 2011), by controlling the microglial production of inflammatory cytokines, and growth factors such as BDNF and ATP (Gomes *et al.*, 2013; George *et al.*, 2015). By taking advantage of a simple paradigm based on the addition of activated N9 microglia releasing ATP, the present study provides evidence that microglia-derived purines in a neuroinflammatory paradigm modulate, via presynaptic $P2X_4Rs$ and A_1Rs, different forms of presynaptic short-term plasticity at MF-CA3 synapses. However, the simplicity of the paradigm used also introduced some limitations in the mechanistic process underlying this control of short-term plasticity by microglia-derived ATP. Indeed, our experimental approach does not allow us to rule out the participation of endogenous microglia, astrocytes and/or neurons in possible amplification of the N9 microglia-derived ATP to control presynaptic short-term plasticity at MF-CA3 synapses. In this

respect, a recent study showed that the production of tumour necrosis factor-α and ATP by microglia was driving nearby astrocytes to release ATP, promoting, in turn, astroglial release of glutamate and a subsequent increase in CA1 synaptic transmission in acute hippocampal slices (Pascual *et al.*, 2012). However, this documented ATP-induced ATP release from astrocytes occurs only for ATP concentrations in the high micromolar range (Anderson *et al.*, 2004), whereas we have previously estimated that N9 microglia release nanomolar concentrations of ATP (George *et al.*, 2015). Certainly, future studies will be required to unravel the intricate interplay between different cell types in the purinergic control of presynaptic short-term plasticity at MF-CA3 synapses triggered by a neuroinflammation-associated increase in the concentration of microglia-derived ATP.

The CA3 subregion of the hippocampus has been reported to be involved in the encoding, storage and subsequent retrieval of memories (Nakazawa *et al.*, 2003; Bischofberger *et al.*, 2006; Kesner, 2007). Owing to the sparse connectivity between dentate gyrus granule cells and CA3 pyramidal neurons and the prominent ability of MF-CA3 synapses to facilitate markedly the MF pathway has been particularly involved in the pattern separation process (Bischofberger *et al.*, 2006; Gilbert & Kesner, 2006; Leutgeb *et al.*, 2007; Neves *et al.*, 2008). Therefore, a decrease in short-term plasticity induced by neuroinflammation could impact on the pattern separation process. Relevant to this, it is well known that murine models of Alzheimer's disease, which show prominent neuroinflammation, have impaired spatial memory, as is also found in Alzheimer's patients. It would be interesting to use behavioural paradigms to test the pattern separation process in mice with conditional deletion of $P2X_4Rs$ and/or A_1Rs in granule cells, in order to test the possible involvement of this subnetwork.

Acknowledgements

The authors wish to thank Catarina V. Gomes for carrying out the initial experiments to optimize the protocol for adhesion of N9 cells to hippocampal slices, François Rassendren for his generous gift of $P2X_4R$ KO mice, Virginie Labrousse for her help with the immunohistochemistry of $P2X_4Rs$, and Eric Boué-Grabot for his help with the pharmacology of $P2X_4Rs$. The microscopy was done in the Bordeaux Imaging Center (BIC), a service unit of the CNRS-Inserm and Bordeaux University, member of the national infrastructure France BioImaging.

Abbreviations

5-BDBD, 5-(3-bromophenyl)-1,3-dihydro-2*H*-benzofuro[3,2-e]-1,4-diazepin-2-one; A_1R, A_1 receptor; $A_{2A}R$, A_{2A} receptor; CCPA, 2-chloro-N^6-cyclopentyladenosine; DPCPX, 8-cyclopentyl-1,3-dipropylxanthine; EPSC, excitatory postsynaptic current; FF, frequency facilitation; KO, knockout; LPS, lipopolysaccharide; LPS-microglia, lipopolysaccharide-treated microglia; MF, mossy fibre; MF-EPSC, mossy fibre-CA3 excitatory postsynaptic current; NDS, normal donkey serum; P, postnatal day; PBS, phosphate-buffered saline; PBST, 0.1 M phosphate-buffered saline with 0.3% Triton X-100; PPADS, pyridoxalphosphate-6-azophenyl-2′,4′-disulfonic acid; PPF, paired-pulse facilitation; PPR, paired-pulse ratio; $P2X_4R$, $P2X_4$ receptor; SEM, standard error of the mean.

References

Anderson, C.M., Bergher, J.P. & Swanson, R.A. (2004) ATP-induced ATP release from astrocytes. *J. Neurochem.*, **88**, 246–256.

Antonio, L.S., Stewart, A.P., Varanda, W.A. & Edwardson, J.M. (2014) Identification of P2X2/P2X4/P2X6 heterotrimeric receptors using atomic force microscopy (AFM) imaging. *FEBS Lett.*, **588**, 2125–2128.

Armstrong, J., Brust, T., Lewis, R. & MacVicar, B. (2002) Activation of presynaptic P2X7-like receptors depresses mossy fiber–CA3 synaptic transmission through p38 mitogen-activated protein kinase. *J. Neurosci.*, **22**, 5938–5945.

Baxter, A.W., Choi, S.J., Sim, J.A. & North, R.A. (2011) Role of P2X4 receptors in synaptic strengthening in mouse CA1 hippocampal neurons. *Eur. J. Neurosci.*, **34**, 213–220.

Ben Achour, S. & Pascual, O. (2010) Glia: the many ways to modulate synaptic plasticity. *Neurochem. Int.*, **57**, 440–445.

Bessis, A., Béchade, C., Bernard, D. & Roumier, A. (2007) Microglial control of neuronal death and synaptic properties. *Glia*, **55**, 233–238.

Bischofberger, J., Engel, D., Frotscher, M. & Jonas, P. (2006) Timing and efficacy of transmitter release at mossy fiber synapses in the hippocampal network. *Eur. J. Physiol.*, **453**, 361–372.

Burnstock, G., Fredholm, B. & Verkhratsky, A. (2011) Adenosine and ATP receptors in the brain. *Curr. Top. Med. Chem.*, **11**, 973–1011.

Butt, A.M. (2011) ATP: a ubiquitous gliotransmitter integrating neuron–glial networks. *Semin. Cell Dev. Biol.*, **22**, 205–213.

Centonze, D., Muzio, L., Rossi, S., Cavasinni, F., De Chiara, V., Bergami, A., Musella, A., D'Amelio, M., Cavallucci, V., Martorana, A., Bergamaschi, A., Cencioni, M.T., Diamantini, A., Butti, E., Comi, G., Bernardi, G., Cecconi, F., Battistini, L., Furlan, R. & Martino, G. (2009) Inflammation triggers synaptic alteration and degeneration in experimental autoimmune encephalomyelitis. *J. Neurosci.*, **29**, 3442–3452.

Contractor, A., Swanson, G. & Heinemann, S. (2001) Kainate receptors are involved in short- and long-term plasticity at mossy fiber synapses in the hippocampus. *Neuron*, **29**, 209–216.

Costenla, A.R., Diógenes, M.J., Canas, P.M., Rodrigues, R.J., Nogueira, C., Maroco, J., Agostinho, P.M., Ribeiro, J.A., Cunha, R.A. & de Mendonça, A. (2011) Enhanced role of adenosine A_{2A} receptors in the modulation of LTP in the rat hippocampus upon aging. *Eur. J. Neurosci.*, **34**, 12–21.

Cunha, R.A. (2001) Regulation of the ecto-nucleotidase pathway in rat hippocampal nerve terminals. *Neurochem. Res.*, **26**, 979–991.

Cunha, R.A., Sebastião, A.M. & Ribeiro, J.A. (1998) Inhibition by ATP of hippocampal synaptic transmission requires localized extracellular catabolism by ecto-nucleotidases into adenosine and channeling to adenosine A_1 receptors. *J. Neurosci.*, **18**, 1987–1995.

Di Virgilio, F., Ceruti, S., Bramanti, P. & Abbracchio, M.P. (2009) Purinergic signalling in inflammation of the central nervous system. *Trends Neurosci.*, **32**, 79–87.

Dias, R., Ribeiro, J. & Sebastião, A. (2012) Enhancement of AMPA currents and GluR1 membrane expression through PKA-coupled adenosine A_{2A} receptors. *Hippocampus*, **22**, 276–291.

Donnelly-Roberts, D., McGaraughty, S., Shieh, C., Honore, P. & Jarvis, M.F. (2008) Painful purinergic receptors. *J. Pharmacol. Exp. Ther.*, **324**, 409–415.

Dunwiddie, T.V. & Masino, S.A. (2001) The role and regulation of adenosine in the central nervous system. *Annu. Rev. Neurosci.*, **24**, 31–55.

Fredholm, B., IJzerman, A., Jacobson, K., Linden, J. & Müller, C. (2011) International Union of Basic and Clinical Pharmacology. Nomenclature and classification of adenosine receptors – an update. *Pharmacol. Rev.*, **63**, 1–34.

Frenguelli, B.G., Wigmore, G., Llaudet, E. & Dale, N. (2007) Temporal and mechanistic dissociation of ATP and adenosine release during ischaemia in the mammalian hippocampus. *J. Neurochem.*, **101**, 1400–1413.

George, J., Gonçalves, F.Q., Cristóvão, G., Rodrigues, L., Meyer Fernandes, J.R., Gonçalves, T., Cunha, R.A. & Gomes, C.A. (2015) Different danger signals differently impact on microglial proliferation through alterations of ATP release and extracellular metabolism. *Glia*, **63**, 1636–1645.

Gilbert, P. & Kesner, R. (2006) The role of the dorsal CA3 hippocampal subregion in spatial working memory and pattern separation. *Behav. Brain Res.*, **169**, 142–149.

Gomes, C., Ferreira, R., George, J., Sanches, R., Rodrigues, D.I., Gonçalves, N. & Cunha, R.A. (2013) Activation of microglial cells triggers a release of brain-derived neurotrophic factor (BDNF) inducing their proliferation in an adenosine A_{2A} receptor-dependent manner: A_{2A} receptor blockade prevents BDNF release and proliferation of microglia. *J. Neuroinflamm.*, **10**, 16.

Gundlfinger, A., Bischofberger, J., Johenning, F.W., Torvinen, M., Schmitz, D. & Breustedt, J. (2007) Adenosine modulates transmission at the hippocampal mossy fibre synapse via direct inhibition of presynaptic calcium channels. *J. Physiol.*, **582**, 263–277.

Jinno, S., Fleischer, F., Eckel, S., Schmidt, V. & Kosaka, T. (2007) Spatial arrangement of microglia in the mouse hippocampus: a stereological study in comparison with astrocytes. *Glia*, **55**, 1334–1347.

Kesner, R. (2007) Behavioral functions of the CA3 subregion of the hippocampus. *Learn Memory*, **14**, 771–781.
Kettenmann, H., Hanisch, U., Noda, M. & Verkhratsky, A. (2011) Physiology of microglia. *Physiol. Rev.*, **91**, 461–553.
Kettenmann, H., Kirchhoff, F. & Verkhratsky, A. (2013) Microglia: new roles for the synaptic stripper. *Neuron*, **77**, 10–18.
Khakh, B.S., Proctor, W.R., Dunwiddie, T.V., Labarca, C. & Lester, H.A. (1999) Allosteric control of gating and kinetics at $P2X_4$ receptor channels. *J. Neurosci.*, **19**, 7289–7299.
Khakh, B.S., Gittermann, D., Cockayne, D. & Jones, A. (2003) ATP modulation of excitatory synapses onto interneurons. *J. Neurosci.*, **23**, 7426–7437.
Koizumi, S., Ohsawa, K., Inoue, K. & Kohsaka, S. (2013) Purinergic receptors in microglia: functional modal shifts of microglia mediated by P2 and P1 receptors. *Glia*, **61**, 47–54.
Kukley, M., Stausberg, P., Adelmann, G., Chessell, I. & Dietrich, D. (2004) Ecto-nucleotidases and nucleoside transporters mediate activation of adenosine receptors on hippocampal mossy fibers by $P2X_7$ receptor agonist 2′-3′-O-(4-benzoylbenzoyl)-ATP. *J. Pharmacol. Exp. Ther.*, **324**, 409–415.
Kukley, M., Schwan, M., Fredholm, B.B. & Dietrich, D. (2005) The role of extracellular adenosine in regulating mossy fiber synaptic plasticity. *J. Neurosci.*, **25**, 2832–2837.
Lambrecht, G., Braun, K., Damer, M., Ganso, M., Hildebrandt, C., Ullmann, H., Kassack, M.U. & Nickel, P. (2002) Structure–activity relationships of suramin and pyridoxal-5′-phosphate derivatives as P2 receptor antagonists. *Curr. Pharm. Des.*, **8**, 2371–2399.
Leutgeb, J., Leutgeb, S., Moser, M. & Moser, E. (2007) Pattern separation in the dentate gyrus and CA3 of the hippocampus. *Science*, **315**, 961–966.
Lopes, L.V., Halldner, L., Rebola, N., Johansson, B., Ledent, C., Chen, J.F., Fredholm, B.B. & Cunha, R.A. (2004) Binding of the prototypical adenosine A_{2A} receptor agonist CGS 21680 to the cerebral cortex of adenosine A_1 and A_{2A} receptor knockout mice. *Br. J. Pharmacol.*, **141**, 1006–1014.
Marchal, C. & Mulle, C. (2004) Postnatal maturation of mossy fibre excitatory transmission in mouse CA3 pyramidal cells: a potential role for kainate receptors. *J. Physiol.*, **561**, 27–37.
Matos, M., Augusto, E., Santos-Rodrigues, A., Schwarzschild, M.A., Chen, J.F., Cunha, R.A. & Agostinho, P.M. (2012) Adenosine A_{2A} receptors modulate glutamate uptake in cultured astrocytes and gliosomes. *Glia*, **60**, 702–716.
Moore, K.A., Nicoll, R.A. & Schmitz, D. (2003) Adenosine gates synaptic plasticity at hippocampal mossy fiber synapses. *Proc. Natl. Acad. Sci. USA*, **100**, 14397–14402.
Nakazawa, K., Sun, L., Quirk, M., Rondi-Reig, L., Wilson, M. & Tonegawa, S. (2003) Hippocampal CA3 NMDA receptors are crucial for memory acquisition of one-time experience. *Neuron*, **38**, 305–315.
Neary, J. & Zimmermann, H. (2009) Trophic functions of nucleotides in the central nervous system. *Trends Neurosci.*, **32**, 189–198.
Neves, G., Cooke, S.F. & Bliss, T.V. (2008) Synaptic plasticity, memory and the hippocampus: a neural network approach to causality. *Nat. Rev. Neurosci.*, **9**, 65–75.
Nicoll, R. & Schmitz, D. (2005) Synaptic plasticity at hippocampal mossy fibre synapses. *Nat. Rev. Neurosci.*, **6**, 863–876.
Pankratov, Y.V., Lalo, U.V. & Krishtal, O.A. (2002) Role for P2X receptors in long-term potentiation. *J. Neurosci.*, **22**, 8363–8369.
Pascual, O., Ben Achour, S., Rostaing, P., Triller, A. & Bessis, A. (2012) Microglia activation triggers astrocyte-mediated modulation of excitatory neurotransmission. *Proc. Natl. Acad. Sci. USA*, **109**, 197–205.
Pougnet, J., Toulme, E., Martinez, A., Choquet, D., Hosy, E. & Boué-Grabot, E. (2014) ATP P2X receptors downregulate AMPA receptor trafficking and postsynaptic efficacy in hippocampal neurons. *Neuron*, **16**, 417–430.
Priel, A. & Silberberg, S. (2004) Mechanism of ivermectin facilitation of human P2X4 receptor channels. *J. Gen. Physiol.*, **123**, 281–293.
Rebola, N., Sebastião, A., de Mendonça, A., Oliveira, C., Ribeiro, J. & Cunha, R.A. (2003) Enhanced adenosine A_{2A} receptor facilitation of synaptic transmission in the hippocampus of aged rats. *J. Neurophysiol.*, **90**, 1295–1303.
Rebola, N., Canas, P., Oliveira, C. & Cunha, R. (2005) Different synaptic andsubsynaptic localization of adenosine A2A receptors in the hippocampus and striatum of the rat. *Neuroscience*, **132**, 893–903.
Rebola, N., Lujan, R., Cunha, R. & Mulle, C. (2008) Adenosine A_{2A} receptors are essential for long-term potentiation of NMDA-EPSCs at hippocampal mossy fiber synapses. *Neuron*, **57**, 121–134.
Rebola, N., Simões, A.P., Canas, P.M., Tomé, A.R., Andrade, G.M., Barry, C.E., Agostinho, P.M., Lynch, M.A. & Cunha, R.A. (2011) Adenosine A_{2A} receptors control neuroinflammation and consequent hippocampal neuronal dysfunction. *J. Neurochem.*, **117**, 100–111.
Rodrigues, R.J., Almeida, T., Richardson, P.J., Oliveira, C.R. & Cunha, R.A. (2005) Dual presynaptic control by ATP of glutamate release via facilitatory $P2X_1$, $P2X_{2/3}$ and $P2X_3$, and inhibitory $P2Y_1$, $P2Y_2$ and/or $P2Y_4$ receptors in the rat hippocampus. *J. Neurosci.*, **27**, 6286–6295.
Rodrigues, R.J., Tomé, A.R. & Cunha, R.A. (2015) ATP as a multi-target danger signal in the brain. *Front. Neurosci.*, **9**, 148.
Roumier, A., Pascual, O., Béchade, C., Wakselman, S., Poncer, J., Réal, E., Triller, A. & Bessis, A. (2008) Prenatal activation of microglia induces delayed impairment of glutamatergic synaptic function. *PLoS One*, **3**, e2595.
Rubio, M.E. & Soto, F. (2001) Distinct Localization of P2X receptors at excitatory postsynaptic specializations. *J. Neurosci.*, **21**, 641–653.
Sachidhanandam, S., Blanchet, C., Jeantet, Y., Cho, Y.H. & Mulle, C. (2009) Kainate receptors act as conditional amplifiers of spike transmission at hippocampal mossy fiber synapses. *J. Neurosci.*, **29**, 5000–5008.
Salin, P., Scanziani, M., Malenka, R. & Nicoll, R. (1996) Distinct short-term plasticity at two excitatory synapses in the hippocampus. *Proc. Natl. Acad. Sci. USA*, **93**, 13304–13309.
Scanziani, M., Capogna, M., Gähwiler, B. & Thompson, S. (1992) Presynaptic inhibition of miniature excitatory synaptic currents by baclofen and adenosine in the hippocampus. *Neuron*, **9**, 919–927.
Sebastião, A.M., Cunha, R.A., de Mendonça, A. & Ribeiro, J.A. (2000) Modification of adenosine modulation of synaptic transmission in the hippocampus of aged rats. *Br. J. Pharmacol.*, **131**, 1629–1634.
Sim, J., Chaumont, S., Jo, J., Ulmann, L., Young, M., Cho, K., Buell, G., North, R. & Rassendren, F. (2006) Altered hippocampal synaptic potentiation in P2X4 knockout mice. *J. Neurosci.*, **26**, 9006–9009.
Soto, F., Garcia-Guzman, M., Gomez-Hernandez, J.M., Hollmann, M., Karschin, C. & Stühmer, W. (1996) P2X4: an ATP-activated ionotropic receptor cloned from rat brain. *Proc. Natl. Acad. Sci. USA*, **93**, 3684–3688.
Sperlágh, B., Köfalvi, A., Deuchars, J., Atkinson, L., Milligan, C., Buckley, N. & Vizi, E. (2002) Involvement of P2X7 receptors in the regulation of neurotransmitter release in the rat hippocampus. *J. Neurochem.*, **81**, 1196–1211.
Toulme, E. & Khakh, B. (2012) Imaging P2X4 receptor lateral mobility in microglia regulation by calcium and p38 MAPK. *J. Biol. Chem.*, **287**, 14734–14748.
Tremblay, M., Lowery, R. & Majewska, A. (2010) Microglial interactions with synapses are modulated by visual experience. *PLoS Biol.*, **8**, e1000527.
Verkhratsky, A., Anderova, M. & Chvatal, A. (2009) Differential calcium signalling in neuronal–glial networks. *Front Biosci.*, **14**, 2004–2016.
Wake, H., Moorhouse, A.J., Jinno, S., Kohsaka, S. & Nabekura, J. (2009) Resting microglia directly monitor the functional state of synapses in vivo and determine the fate of ischemic terminals. *J. Neurosci.*, **29**, 3974–3978.
Xiang, Z. & Burnstock, G. (2005) Expression of P2X receptors on rat microglial cells during early development. *Glia*, **52**, 119–126.
Xu, J., Chai, H., Ehinger, K., Egan, T.M., Srinivasan, R., Frick, M. & Khakh, B.S. (2014) Imaging P2X4 receptor subcellular distribution, trafficking, and regulation using P2X4-pHluorin. *J. Gen. Physiol.*, **144**, 81–104.
Yu, Y., Ugawa, S., Ueda, T., Ishida, Y., Inoue, K., Kyaw Nyunt, A., Umemura, A., Mase, M., Yamada, K. & Shimada, S. (2008) Cellular localization of P2X7 receptor mRNA in the rat brain. *Brain Res.*, **1194**, 45–55.
Zemkova, H., Khadra, A., Rokic, M.B., Tvrdonova, V., Sherman, A. & Stojilkovic, S.S. (2015) Allosteric regulation of the P2X4 receptor channel pore dilation. *Pflug. Arch.*, **467**, 713–726.